ISSN 0021-3640, JETP Letters, 2020, Vol. 111, No. 12, pp. 690–693. © Pleiades Publishing, Inc., 2020.
Russian Text © The Author(s), 2020, published in Pis'ma v Zhurnal Eksperimental'noi i Teoreticheskoi Fiziki, 2020, Vol. 111, No. 12, pp. 815–818.

CONDENSED MATTER

Magnetoelectric Effect in CoFeB/MgO/CoFeB Magnetic Tunnel Junctions

I. Yu. Pashen'kin[a, *], M. V. Sapozhnikov[a, b], N. S. Gusev[a], V. V. Rogov[a], D. A. Tatarskii[a, b], A. A. Fraerman[a], and M. N. Volochaev[c]

[a] *Institute for Physics of Microstructures, Russian Academy of Sciences, Nizhny Novgorod, 603950 Russia*
[b] *Lobachevsky State University of Nizhny Novgorod, Nizhny Novgorod, 603950 Russia*
[c] *Kirensky Institute of Physics, Siberian Branch, Russian Academy of Sciences, Krasnoyarsk, 660036 Russia*
**e-mail: pashenkin@ipmras.ru*

Received April 27, 2020; revised May 1, 2020; accepted May 1, 2020

The possibility of electrical control of the interlayer exchange interaction in CoFeB/MgO/CoFeB tunnel junctions exhibiting magnetoresistance of ~200% is studied. It is shown that the increase in the applied voltage from 50 mV to 1.25 V leads to a shift of the magnetization curve of the free layer by 10 Oe at a current density of ~10^3 A/cm^2. The discovered effect can be used in the development of energy-efficient random access memory.

DOI: 10.1134/S0021364020120115

One of the most urgent practically significant problems of spin electronics is to control the magnetic state of nanosystems by the electric field (magnetoelectric effect), i.e., without the application of high-density currents. The use of the magnetoelectric effect ensures the high recording density and energy efficiency of magnetoresistive random access memory (MRAM). The MRAM element is a tunnel magnetoresistive (TMR) junction, the logical state (resistance) of which is determined by the mutual orientation of the magnetizations of the free (soft magnetic) and fixed (hard magnetic) layers. Recording information into a cell involves the magnetization reversal of its free layer, which is a nontrivial task. In the first commercially available MRAMs, switching was performed by the magnetic fields of the recording current buses [1, 2]. When moving to the nanoscale, this approach turns out to be extremely inefficient because of a high heat release and the impossibility of localizing magnetic fields. Currently, the recording process is based on the application of spin polarized currents of very high densities (~10^6 A/cm^2) to a system [3, 4], inevitably leading to significant energy loss. Magnetization reversal caused by the dependence of magnetic anisotropy on the applied voltage [5, 6] does not require high currents, but in view of the quadratic dependence of the effect on magnetization, the deterministic switching is possible only in the dynamic mode, which imposes strict requirements on the duration and shape of voltage pulses. The controlled anisotropy effect is also used to assist magnetization reversal by a spin-polarized current [7], but the switching barrier decreases only in one direction (e.g., from 0 to 1) because the effect is an even function of the voltage.

The dependence of the interlayer exchange interaction on the voltage [8] applied to the TMR junction allows deterministic switching at a relatively low current density passing through the system. This effect is due to the change in the shape of the potential barrier under the effect of the electric field and, as a consequence, the change in its tunnel transparency, which determines the exchange constant. In this work, we studied the possibility of controlling the interlayer exchange interaction by applying the electric voltage to the CoFeB/MgO/CoFeB TMR junctions. This system demonstrates the giant tunneling magnetoresistance [9] and is the most promising for the development of MRAM.

Multilayer Ta(20 nm)/Pt(10 nm)/Ta(20 nm)/CoFeB(3–5 nm)/MgO(1.3–1.5 nm)/CoFeB(5 nm)/IrMn(10 nm)/Ta(3 nm)/Pt(10 nm) nanostructures grown on Si/SiO_2 substrates by high-vacuum magnetron sputtering at room temperature were used to manufacture TMR elements. The residual pressure in the growth chamber did not exceed 3×10^{-7} Torr, and the working argon pressure during the deposition was $(1.5–2) \times 10^{-3}$ Torr. The MgO barrier layer was formed by the rf sputtering of a MgO stoichiometric dielectric target. Using successive optical lithography and ion etching, 1.5 × 4-μm rectangular multilayer particles were made from the resulting structures. Then, the TMR junctions were connected in series in chains of 50 elements with gold bridges to prevent static breakdown and junction pads were formed for

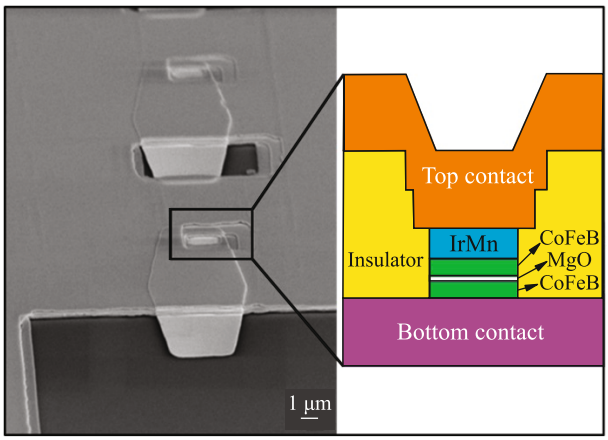

Fig. 1. (Color online) (Left panel) Scanning electron microscopy image of a region of a chain of TMR junctions and (right panel) the schematic of the cross section (perpendicular to the chain) of a TMR junction.

connection to a measuring circuit. Figure 1 shows a scanning electron microscopy image of a part of a chain of TMR elements obtained prior to the upper contact deposition step, as well as a schematic image of a TMR junction built into the electrode system.

The final manufacturing stage was the thermal annealing of the prepared chips in vacuum at 330°C for 2 h, which results in a significant increase in the TMR effect from 10–20 to 100–200% for different samples (Fig. 2), which corresponds to the world level in the field of magnetoresistive structures [10]. The decrease in the unidirectional anisotropy in the fixed layer of annealed structures is probably due to the diffusion of Mn atoms from the antiferromagnetic IrMn layer and the violation of the quality of the CoFeB/IrMn interface.

The increase in the magnetoresistance during annealing is associated with the recrystallization of amorphous CoFeB layers from the interface with the MgO [001] textured barrier, which, in turn, imposes the [001] crystallographic orientation on the ferromagnetic layers. The MgO layer itself initially acquires a crystal structure oriented in the [001] direction upon sputtering on an amorphous CoFeB layer. The presence of the crystal texture of the MgO [001] and CoFeB [001] layers is a prerequisite for observing the giant TMR effect in this system because of the features of the band structure of these materials [11].

The resolution of the electron microscopy image of the cross section of the TMR structures (Fig. 3) is insufficient to determine the specific crystal structure and orientation of the CoFeB and MgO layers, but it is sufficient to distinguish between polycrystalline and amorphous materials. It is seen in Fig. 3 that, after thermal annealing, an inhomogeneous polycrystalline contrast appeared in CoFeB layers (Fig. 3b), which

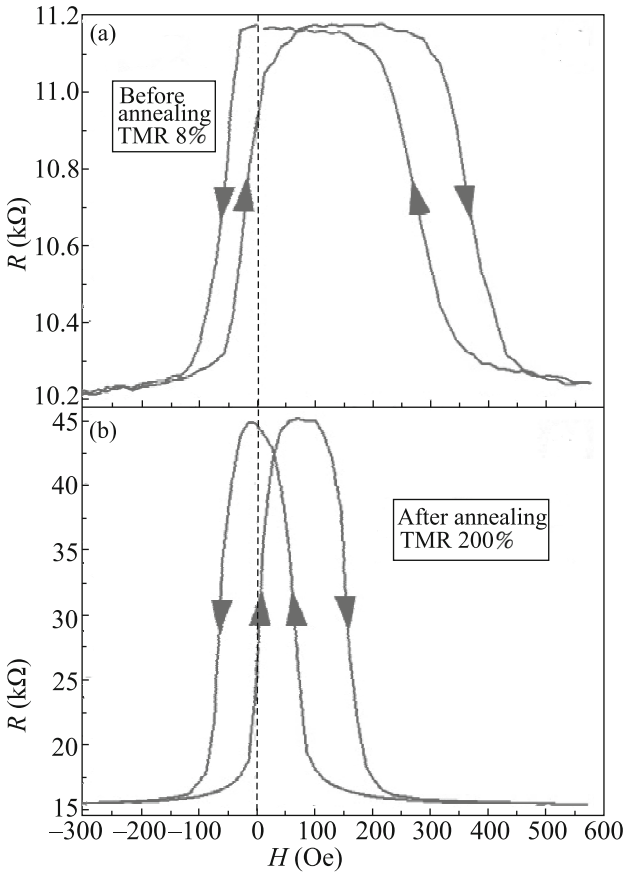

Fig. 2. Magnetoresistance curves of the chain of CoFeB/MgO/CoFeB TMR junctions (a) before and (b) after thermal annealing.

was initially absent in amorphous CoFeB layers (Fig. 3a).

In order to clarify the possibility of electrical control of the interlayer exchange interaction, magnetotransport measurements were carried out at various voltages applied to the chains and individual TMR junctions (Fig. 4). As a result, it was found that the increase in the voltage leads to a significant drop in the TMR effect (Figs. 4a, 4c), which is typical of the studied system and was observed earlier [12]. It is more important that the increase in the applied voltage from 50 mV to 1.25 V (which corresponds to the electric field of $\approx 10^9$ V/m) by one junction is accompanied by a shift of the magnetization curve of the free layer by up to 10 Oe (Figs. 4b, 4d), which indicates the change in the exchange interaction between the magnetic layers. In this case, the current flowing through the junction has a density of about 10^3 A/cm^2 (at the voltage of 1.25 V per junction), which is two or three orders of magnitude lower than the currents necessary for switching of the MRAM cell due to the spin-transfer torque effect (STT-MRAM). It should be noted that the magnitude of the TMR effect, as well as the shape

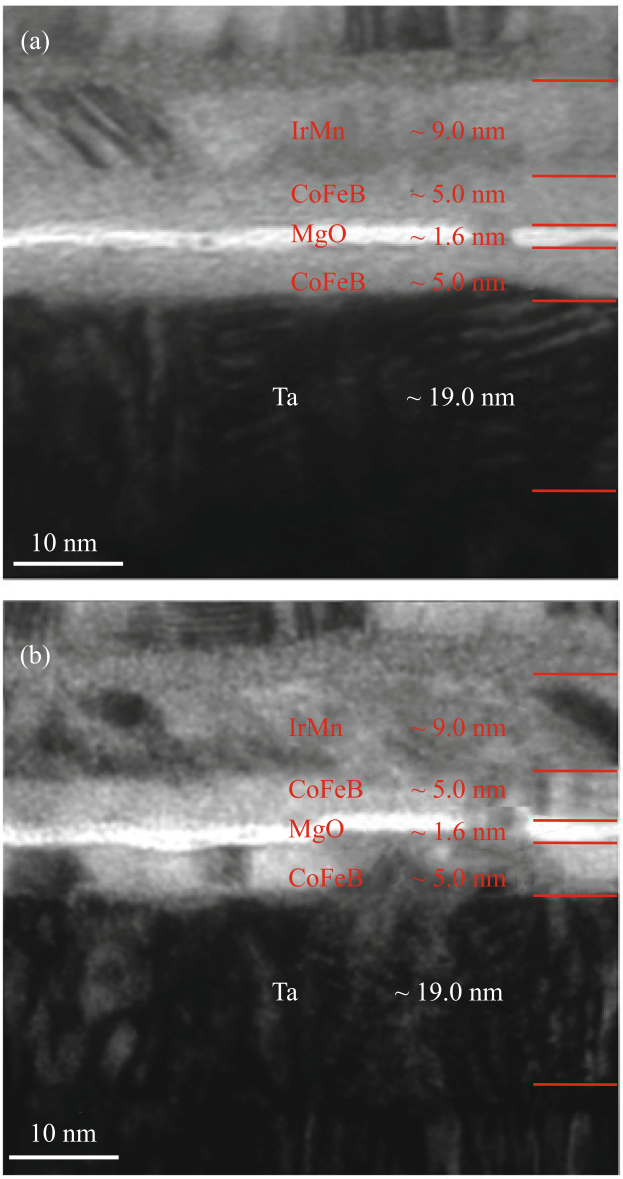

Fig. 3. (Color online) Transmission electron microscopy images of the cross section of the CoFeB/MgO/CoFeB TMR structure (a) before and (b) after thermal annealing.

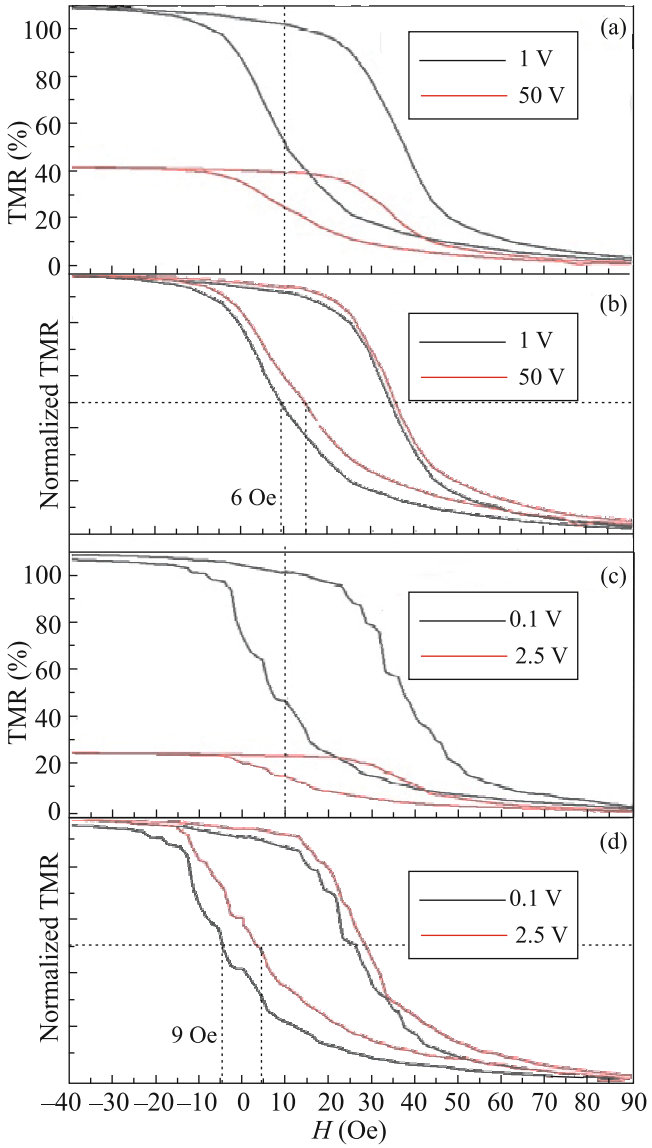

Fig. 4. (Color online) Magnetoresistance curves for (a, b) chains of TMR junctions and (c, d) pairs of TMR junctions at various applied voltages.

and position of the magnetoresistance curves, is completely recovered at the decrease in the voltage.

To effectively switch the state of the TMR element, the field shift should be larger than the slope width of the hysteresis curve, which is 20–30 Oe for different samples. The study of magnetoresistive curves of single junctions shows that a wide magnetization reversal front is caused by the appearance of inhomogeneous (multivortex and/or multidomain) states in each individual junction because of micron sizes rather than by the dispersion of particle parameters in the chain. The observed steps on the magnetoresistance curve of a pair of TMR junctions (Figs. 4c, 4d) are due to the transition of the system through a sequence of metastable inhomogeneous magnetic states during the magnetization reversal of the system. The increase in the steepness of magnetoresistive curves can be achieved by the electron lithography fabrication of submicron (200–300 nm) TMR elements. Magnetic particles of this size will have two stable states with a uniform distribution of magnetization, switching between which occurs stepwise [13].

To summarize, the possibility of electrical control of the interlayer exchange interaction in the CoFeB/MgO/CoFeB system has been experimentally demonstrated. The resulting TMR junctions exhibit a magnetoresistance of 200% and are highly resistant to

electrical breakdown, which allows applying voltages up to 1.25 V per cell. In this case, a shift of the magnetization curve of the free layer by up to 10 Oe is detected at a current density flowing through the system, ~10^3 A/cm^2. This effect can be used to develop energy-efficient MRAM.

ACKNOWLEDGMENTS

We are grateful to O.G. Udalov for useful discussions.

FUNDING

This work was supported by the Russian Science Foundation (project no. 16-12-10340P).

REFERENCES

1. T. W. Andre, J. J. Nahas, C. K. Subramanian, B. J. Garni, H. S. Lin, A. Omair, and W. L. Martino, IEEE J. Solid-State Circuits **40**, 301 (2005).
2. B. N. Engel, J. Akerman, B. Butcher, R. W. Dave, M. DeHerrera, M. Durlam, G. Grynkewich, J. Janesky, S. V. Pietambaram, N. D. Rizzo, J. M. Slaughter, K. Smith, J. J. Sun, and S. Tehrani, IEEE Trans. Magn. **41**, 132 (2005).
3. S.-C. Oh, S.-Y. Park, A. Manchon, M. Chshiev, J.-H. Han, H. -W. Lee, J.-E. Lee, K.-T. Nam, Y. Jo, Y.-C. Kong, B. Dieny, and K.-J. Lee, Nat. Phys. **5**, 898 (2009).
4. J. C. Sankey, Y.-T. Cui, J. Z. Sun, J. C. Slonczewski, R. A. Buhrman, and D. C. Ralph, Nat. Phys. **4**, 67 (2007).
5. J. G. Alzate, P. Kh. Amiri, P. Upadhyaya, S. S. Cherepov, J. Zhu, M. Lewis, R. Dorrance, J. A. Katine, J. Langer, K. Galatsis, D. Markovic, I. Krivorotov, and K. L. Wang, in *Proceedings of the 2012 International Electron Devices Meeting IEDM 2012, San Francisco, CA, December 10–13, 2012* (IEEE, Piscataway, NJ, 2012), p. 2.5.1.
6. J. G. Alzate, P. Kh. Amiri, G. Yu, P. Upadhyaya, J. A. Katine, J. Langer, B. Ocker, I. N. Krivorotov, and K. L. Wang, Appl. Phys. Lett. **104**, 112410 (2014).
7. W.-G. Wang, M. Li, S. Hageman, and C. L. Chien, Nat. Mater. **11**, 64 (2012).
8. T. Newhouse-Illige, Y. Liu, M. Xu, et al., Nat. Commun. **8**, 15232 (2017).
9. S. Ikeda, J. Hayakawa, Y. Ashizawa, Y. M. Lee, K. Miura, H. Hasegawa, M. Tsunoda, F. Matsukura, and H. Ohno, Appl. Phys. Lett. **93**, 082508 (2008).
10. P. P. Freitas, R. Ferreira, and S. Cardoso, Proc. IEEE **104**, 1894 (2016).
11. S. Yuasa and D. D. Djayaprawira, J. Phys. D: Appl. Phys. **40**, R337 (2007).
12. D. D. Djayaprawira, K. Tsunekawa, M. Nagai, H. Maehara, S. Yamagata, N. Watanabe, S. Yuasa, Y. Suzuki, and K. Ando, Appl. Phys. Lett. **86**, 092502 (2005).
13. S. N. Vdovichev, B. A. Gribkov, S. A. Gusev, A. Yu. Klimov, V. L. Mironov, I. M. Nefedov, V. V. Rogov, A. A. Fraerman, and I. A. Shereshevskii, JETP Lett. **94**, 386 (2011).

Translated by L. Mosina